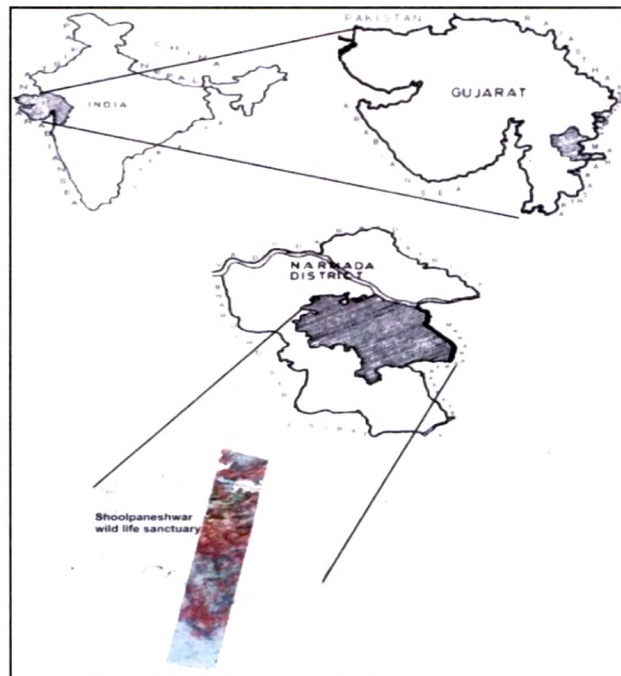


CHAPTER 2

**Materials and Methods**

## 2.1 Study area

The study was conducted in tropical dry deciduous forests of Shoolpaneshwar Wildlife Sanctuary (SWS) located at 21°29'–21°52'N lat. and 73°29'–73°54'E long., Narmada district, Gujarat, India (**Figure 2.1**). Geographically SWS is situated between Karjan river (North) and Narmada river (west). Two major dams (Karjan dam and sardar sarovar dam) were constructed on these rivers which are situated in the peripheral area of the sanctuary (**Figure 2.2**). The sanctuary was first created in 1982 over an area of 150.87 km<sup>2</sup> as "Dumkhal Sanctuary"- an important home for sloth bears. Subsequently, in 1987 and 1989, the area of the sanctuary was enlarged to 675 km<sup>2</sup> and it was renamed as "Shoolpaneshwar Sanctuary". Hilly tract of the Sanctuary bordering Narmada supports some of the best forests in Gujarat. The area is highly important because it forms the catchments area of Karjan and Sardar sarovar reservoir. The SWS is one of the important protected areas supporting sizeable biota. The sanctuary remains covered with lush green vegetation in monsoon and shows dry vegetative condition in summers (**Figure 2.3 and 2.4**).



**Figure 2.1. Location of the study area**

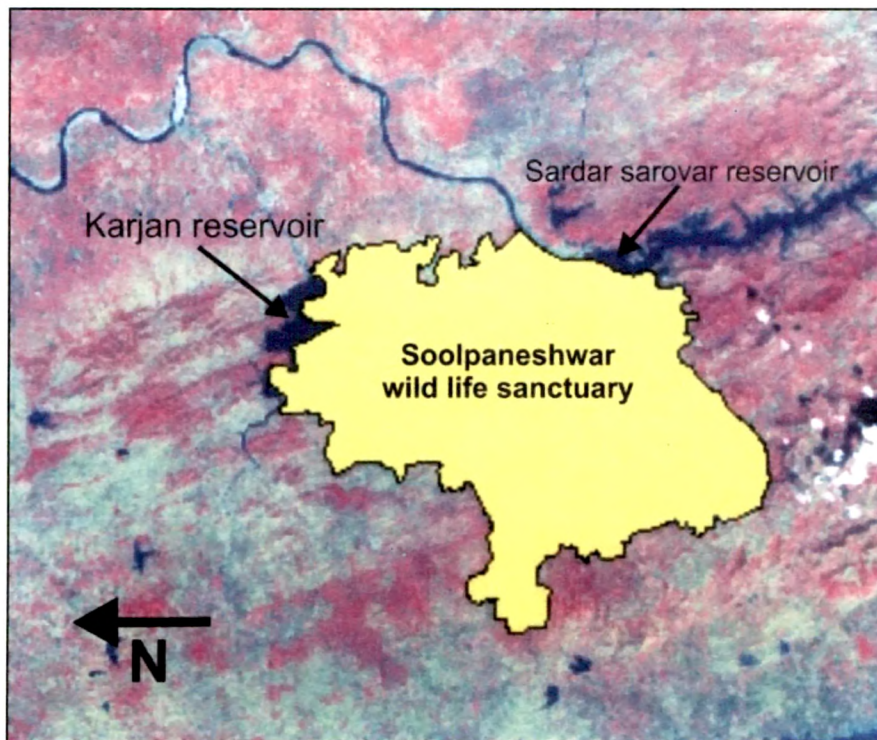


Figure 2.2. Map showing study area



Figure 2.3. SWS in the month of October



**Figure 2.4. SWS in the month of April**

## **2.2 Geology and soil**

Topography of the area is undulating with both continuous and discontinuous hilly tracts up to an elevation of ~800 m intermingled with valleys, streams and sporadic clearings for agriculture. Landscapes culminate at the congregation of Vindhyan-Satpura hill ranges. Dhamanmal, the highest peak located in the eastern portion, is about 882 m in altitude. The general slope of the area is towards the west. Vindhyan-Satpura ranges run in east- west direction diagonally across the country and separates the deccan peninsular plateau in the south from the northern Indo-Gangetic plains. The principal geological formations of this area are Bagh limestone and sand stone, the deccan trap lava flows and alluvial deposits (Sabnis and Amin, 1992). Geologically study area includes the Precambrian basement metamorphics and granites, cretaceous Bagh beds and their fresh water equivalents, deccan trap and associated intrusive, tertiary sedimentary deposits and quaternary alluvium (Deota, 1991). Rocks in SWS are impervious to water and exert considerable influence on the hydrology of the area (Sabnis and

Amin, 1992). The soils in this area vary in colour, texture, depth and the stoniness depending upon the base rock and topography. The light grey, yellowish brown and reddish brown coloured soils were found in the gentle slopes, hill tops and modulating plains of the study area. Alluvium deposits of clay-loam type are also seen with light brown to grey / black colour (Gujarat state forest department unpublished data). The soils at the study area are classified as Entisols (Merh, 1995). Eastern region of the SWS have rocky out crops with well drained calcareous loamy soils. Western part of the SWS is characterized by excessively drained, mixed calcareous and fine montmorillonitic soils with few patches of mixed calcareous and fine loamy soils (NBSS, 1994).

### **2.3 Climatic conditions**

The climate of the sanctuary is periodical with three well defined seasons, winter (November–February), summer (March-June), monsoon (July-October). The temperature in the SWS fluctuates from minimum of 23° to maximum of 44°C in summers and minimum of 10° C and maximum of 30°C in Winters. Winters are cold and dry. January is the coldest part of the year. The summer season is predominantly hot and long. The hottest month of the year is May. The streams and rivers of the study area begin to dry up by mid January and by February very few of them have any water flow. Monsoon season experiences good amount of rainfall. The SWS is under the south west monsoon regime and it rains between June end to September end period (Sabnis and Amin, 1992). Annual rainfall of the area is in the range of 900-1200 mm. Humidity levels are maximum in the monsoon (July- October) and between 15-30 % (dry environments) for the rest of the year. Influence of seasonal variation is seen on the vegetation cover.

## 2.4 Vegetation

The SWS is one of the important protected areas supporting sizeable biota. According to revised system of forest classification proposed by Champion and Seth (1968), the forest in this area are placed in two major types,

### (1.) Moist , mixed deciduous

The moist mixed deciduous forest is generally confined to valleys and plains having good soil moisture. The canopy cover is almost closed and leaf less period begins by the end of the cold season (Sabnis and Amin, 1992). The trees have broad canopy, stout branched trunks and matching roots to hold them firmly to the ground. Many of the trees shed their leaves in the dry season. Smaller trees and shrubs are also seen. Ground cover is predominant during monsoon. Following tree species are commonly found inside moist, mixed deciduous forest of SWS.

*Adina cordifolia* Willd.

*Albizia lebbek* (L.) Willd.

*Anogeissus latifolia* (Roxb.)

*Bauhinia recemosa* (Linn.)

*Butea monosperma* (Roxb.)

*Dalbergia latifolia* (Roxb.)

*Holarrhena pubescens* R. Br.

*Hymenodictyon excelsum* (Roxb.) Wall.

*Largestroemia lanceolata* Wall.

*Meyna laxiflora* Robyns.

*Mitragyna parviflora* Korth.

*Randia brandisii* Gamble.

*Terminalia crenulata* Roth.

## (2.) Dry, mixed deciduous forest

It is commonly found in areas with poor soil cover and heavy biotic pressure (Sabnis and Amin, 1992). The canopy of the trees does not normally exceed 25 meters. Most of the species are deciduous during the summer season. The lower canopy in these forests is also deciduous with occasional evergreens or sub- greens being present in the moist areas. Usually there is an undergrowth of shrubs, but the light reaches the ground allowing the growth of grass occasionally. Following tree species are commonly found in dry, mixed- deciduous forest of SWS.

*Dendrocalamus strictus* (Roxb.) Nees. [Grass species]

*Tectona grandis* L.

*Aegle marmelos* L. (Corr.)

*Bridelia retusa* L.

*Butea monosperma* Lamk.

*Emblica officinalis* Gaertn.

*Garuga pinnata* Roxb.

*Holarrhena pubescens* R. Br.

*Lannea coromandelica* Houtt.

*Madhuca indica* Gmel.

The forests of SWS are known for its rich biodiversity. A large area is occupied by *Tectona grandis* L. (Teak) , *Dendrocalamus strictus* (Roxb.) Nees. (Bamboo) and mixed patches of other species (Pradeepkumar, 1993). Much of the vegetation is modified due to the influence of the biotic pressure and forestry operations. Teak is the principal species. Patches of pure bamboo dominate the western and north-western parts. Teak and Bamboo are the most dominant species of the study area (**Figure 2.5**). Other major vegetation covers include mixed vegetation and agriculture land (**Figure 2.6**). Pure patches of trees such as *Madhuca indica* (Gmel.), *Ficus glomerata*( L.) and *Pongamia pinnata* ( L.) found intermingled with mixed vegetation covers. Trees such as *Pongamia pinnata* (L.) and *Ficus glomerata* (L.) found to be growing near rivers and streams where soil moisture is very high. Mango trees (*Mangifera indica* L.) found to be growing near human settlements

**(Figure 2.7).** Mahudo (*Madhuca indica* Gmel.) found to be growing in the forest area as well as near human settlements. The forest area is intermixed with tribal settlements. Parts of the sanctuary area are cleared by tribals for agriculture. Variation in phenological state is clearly seen among different types vegetation. Very distinct phenological changes occur in deciduous species such as *Tectona grandis* L. (Teak) and *Dendrocalamus strictus* (Roxb.) and *Madhuca indica* Gmel. Leaf shedding in deciduous species starts from December-January and it shows complete leaf shedding in March-April. In evergreen trees like *Mangifera*, *Ficus* and *Pongamia* complete shedding is not seen. These trees appear greener throughout the year. During monsoon and post monsoon periods (upto October) the undergrowths of herbaceous vegetation become more predominant and entire area of the sanctuary gives the impression of semi-evergreen type of forest. Many species of shrubs and herbs are reported from SWS (Sabnis and Amin, 1992). List of few important shrubs and herbs growing in SWS is given below.

### **Shrubs**

*Azanza lampas* Cav.  
*Carvia callosa* (Nees.) Bremek.  
*Desmodium gangeticum* L.  
*Eranthemum roseum* (Vahl) R.Br.  
*Helicteres isora* L.  
*Moghania strobilifera* L.  
*Pogostemon parviflorus* Benth.  
*Wrightia tinctoria* (Roxb.) R. Br.

### **Herbs**

*Abrus precatorius* L.  
*Achyranthus aspera* L.  
*Borreria stricta* L.f.  
*Combratum ovalifolium* Roxb.  
*Cryptolepis buchanani* (Roem. & Schult)  
*Discorea bulbifera* L.  
*Pueraria tuberosa* (Roxb. ex Willd.)

*Sida cordata* Burm.f.

*Vantilago denticulata* Willd.

## **2.5 Ecology**

Sabnis and Amin, (1992) classified the SWS into 8 distinct eco-grade systems according to disturbance and/or degradation level. The first three grades (referred as relatively better ecosystems) occupy 329 Km<sup>2</sup>. and the rest (referred as deteriorating ecosystems) account for about 346 Km<sup>2</sup>. The damaged ecoregions are largely distributed along northern and eastern boundaries of the sanctuary. This area also has a fair amount of human population along with live stock. Few ethnic tribes are staying in the sanctuary for many decades. The degradation in the sanctuary area has started from the peripheral areas and moving towards the interior areas. In the interior areas the tribals started clearing the forest areas for doing agriculture practices.



*Tectona*



*Dendrocalamus*

**Figure 2.5. Two dominant vegetation covers in SWS**



**Less dense**



**Highly dense**

**Figure 2.6. Mixed vegetation covers in SWS**



***Mangifera***



***Madhuca***

**Figure 2.7. *Mangifera* and *Madhuca* vegetation covers**

## 2.6 Hyperion (EO-1) sensor

The NASA New Millennium Program's Earth Observation-1 (EO-1) satellite was successfully launched on 21<sup>st</sup> November 2000 (**Figure 2.8**). There are three primary instruments on the EO-1 spacecraft: the multispectral Advanced Land Imager (ALI), the hyperspectral Hyperion sensor, and the Linear Etalon Imaging Spectrometer Array (LEISA) Atmospheric Corrector (LAC). The EO-1 platform was positioned on orbit to be approximately one minute behind the Landsat 7 Enhanced Thematic Mapper Plus (ETM+) sensor at an altitude of 705 km (Pearlman et al., 2001). **Table 2.1** summarizes the essential spatial and spectral characteristics of the EO-1 instrument suite. **Figure 2.9** illustrates the overlap in surface area coverage of the ALI, Hyperion, and LAC sensors, compared to the Landsat 7 ETM+ ground track (Ungar, 2002). Hyperion is a grating imaging spectrometer providing 10 nm (sampling interval) contiguous bands in the solar reflected spectrum from 400 to 2500 nm with a spatial resolution of 30 m (the same as the ALI and Landsat sensors) over a 7.7 km swath. Each swath, or line of data, contains 256 pixels. The Hyperion has two spectrometers, one VNIR spectrometer and one SWIR spectrometer.

## 2.7 Data acquisition

EO-1 Hyperion data for SWS was obtained on April 09, 2006 and October 21, 2006 (**Figure 2.10**). Selected dates reflect seasonal variability in the data sets. In the month of April, vegetation was in different stages of senescence whereas in the month of October, vegetation was lush green due to monsoon. At the time of the satellite flight, the study area was showing < 25% cloud cover. Hyperion image was acquired in such a way that it covers maximum area of the sanctuary with diverse ecological features. Care was taken to include all major vegetation classes in the acquired Hyperion image.

**Table 2.1. Attributes of Hyperion (EO-1) instrument**

<b>Parameter</b>	<b>Hyperion</b>
Volume (L x W x H, cm)	75 x 39 x 65
Weight (Kg)	49
Average Power (W)	51
Aperture (cm)	12
IFOV	0.043
Cross track FOV (deg)	0.63
Wavelength Range (nm)	400-2500
Spectral Resolution (nm)	10
Number of Spectral Bands	242
Digitization (bits)	12
Frame Rate (Hz)	223.4

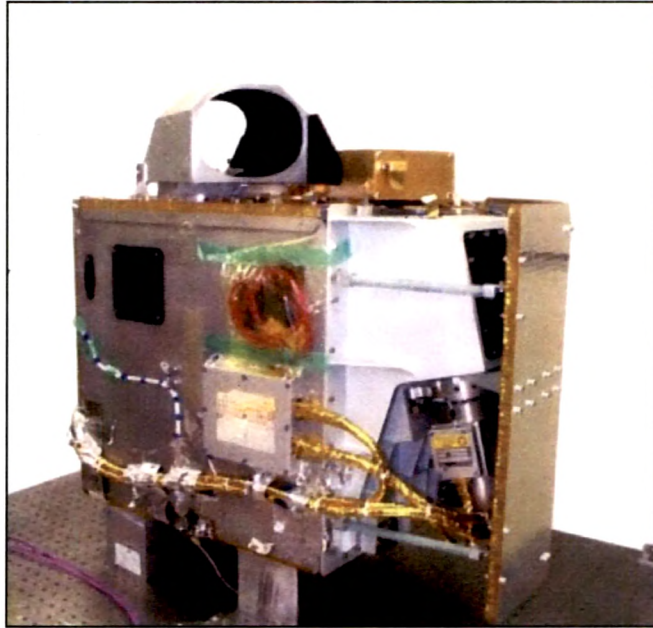


Figure 2.8. EO-1 along with Hyperion instrument (USGS, 2011)

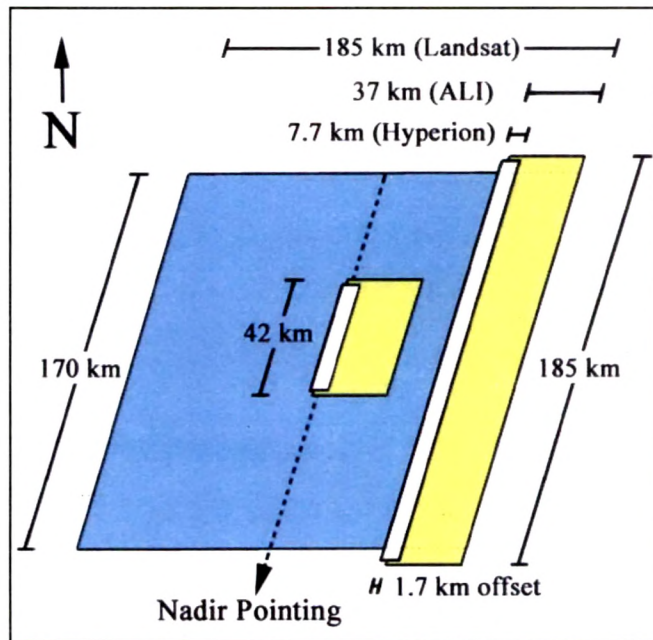


Figure 2.9. Overlap in surface area coverage of the ALI, Hyperion, and LAC sensors (USGS, 2010)



9<sup>th</sup> APRIL



21<sup>st</sup> OCTOBER

**Figure 2.10. False colour composite (FCC) of acquired Hyperion images for two different seasons (559nm, 630nm and 844 nm)**

## 2.8 Radiometric correction of Hyperion image

Radiometric correction of acquired Hyperion images (for the months of April and October) were carried out as reported by Christian and Krishnayya (2007). The Level 1R radiometrically corrected Hyperion product was supplied by the EO-1 Product Generation System (EPGS). The primary function of the EPGS is to perform radiometric calibration and nominal artifact corrections on the level 0 ('raw') Hyperion data. Level 1R algorithms include many processing steps like pre-1R corrections (SWIR only), background removal, rescaling for DN output, bad pixel mask generation, VNIR/SWIR alignment and output data preparation. The Level 1R algorithm output is provided in scaled at-sensor radiance values, with data stored as 12-bit signed integers. The radiance units are in  $W/(sq.mSr \times \mu m)$ . The Level 1R data output needs to be rescaled by the user to obtain the original radiance values. The data were scaled by 40 for the VNIR and 80 for the SWIR to convert the Level 1R data to units of radiance. The first 70 bands were in the VNIR in the spectral range from 356 to 1058 nm with an average full-width at half maximum (FWHM) of 10.90 nm and stored as  $1.80 \times 40 \times DN$  in  $W/(sq. mSr \times \mu m)$ . The remaining 172 bands were in the SWIR, and ranged from 852 to 2577 nm, within average FWHM of 10.14 nm. They were stored as  $1.18 \times 80 \times DN$  in  $W/(sq. mSr \times \mu m)$ . Full dataset has 256 pixels and 6460 lines, with the pixel size of 30 m. The data, with 12-bit quantization, were stored in HDF format as signed 16-bit integers with BIL interleaving (Christian and Krishnayya, 2007).

## 2.9 Atmospheric correction of Hyperion image

There are number of atmospheric agents which contaminate the content of various bands information. Earth's atmosphere contains  $CO_2$ ,  $O_2$ ,  $O_3$ ,  $H_2O$ ,  $CH_4$ ,  $CO$ ,  $NH_4$ ,  $N_2O$ , and other nitrogen gasses, which interact with approximately 50% of the electro magnetic radiation spectrum over the region of 300-2500 nm (Gao and Goetz, 1990; Gao et al., 1993). The gasses and particles in the atmosphere absorb and scatter significant amounts of the electro magnetic radiation over this region (**Figure 2.11**). Atmospheric correction is often

considered as a critical pre-processing step to achieve full spectral information from every pixel especially with hyperspectral data. Even though hyperspectral data have ability to distinguish surface materials especially in geology, agriculture and forestry, there exists a need for preprocessing stages such as atmospheric correction to get reliable and accurate results. During the atmospheric correction, raw radiance data from imaging spectrometer is re-scaled to reflectance data. Therefore, all spectra are shifted to nearly the same albedo. The resultant spectra can be compared with the reflectance spectra of the laboratory or field spectra.

There are many software programs available for atmospheric correction of hyperspectral images including ATREM (Gao and Goetz, 1990; Gao et al., 1992) ACORN (Atmospheric Correction Now) (Analytical Imaging and Geophysics LLC, 2002; Miller, 2002) HyCorr (Hyperspectral Correction), HATCH (High-Accuracy Atmosphere Correction for Hyperspectral Data) (Qu et al., 2000; Goetz, 2002) and FLAASH (Fast Line-of-sight Atmospheric Analysis of Spectral Hypercube) (Goetz, 2002). MODTRAN (Berk et al., 1989; Berk et al., 1998) and LOWTRAN (Kneizys et al., 1988), which operate in a similar manner to ATREM, but use additional ground based measurements to characterize the thermal structure and water content of the atmosphere (Aspinall et al., 2002).

In the present study Atmospheric correction of EO-1 Hyperion image was done using Atmospheric CORrection Now (ACORN 1.5) software. ACORN 1.5 is stand-alone software which is developed for atmospheric correction of hyperspectral and multispectral imageries. ACORN 1.5 is based on MODTRAN 4 radiative transfer code. The Atmospheric Correction Now (ACORN 1.5) software offers a range of options for atmospherically correcting hyperspectral and multispectral remote sensing data sets. In specific modes of operation, ACORN 1.5 uses radiative transfer calculations and the measured, calibrated hyperspectral data to deduce a subset of the atmospheric properties present in the hyperspectral data set. These derived atmospheric properties are used with modeled atmospheric properties to correct the hyperspectral data set. With an input of calibrated hyperspectral

radiance data, ACORN 1.5 produces an output of apparent surface reflectance. The hyperspectral data must be spectrally and radiometrically calibrated to use ACORN 1.5. The ACORN 1.5 user controls the strategy for water vapor estimation, artifact suppression and visibility constraint and estimation. Atmospheric correction in this study was carried out using ACORN 1.5, which includes atmospheric correction of hyperspectral data with water vapor and liquid water spectral fitting for push broom sensors. The resulting spectra were compared with original ones. Atmospheric correction was done on 196 bands after excluding the other 46 non-calibrated and overlapped bands.

## **2.10 Geometric registration of Hyperion image**

The generally accepted procedure for geometric registration is to match a set of points on one image to those on the other. The coordinates from this set of points are then used to calculate a transformation function that will change the coordinates of one image and make it match, geometrically, with the other image. This is referred to as ground control point (GCP) registration. Major Road forkings, Bridges or canals were used as GCPs. Geometric registration was done using ERDAS Imagine V.8.7. Hyperion images were rectified to a common projection (geographic spheroid WGS 84) using well-identified GCPs. The resultant rectified Hyperion image had 0.1 pixels RMSE (Root Mean Square Error). A subset was extracted from October and April Hyperion images (an area of 67.5 km<sup>2</sup>) coinciding exactly with the one covered in field survey (**Figure 2.12 and 2.13**). Subset extraction and image processing was performed by using ENVI 4.6 software.

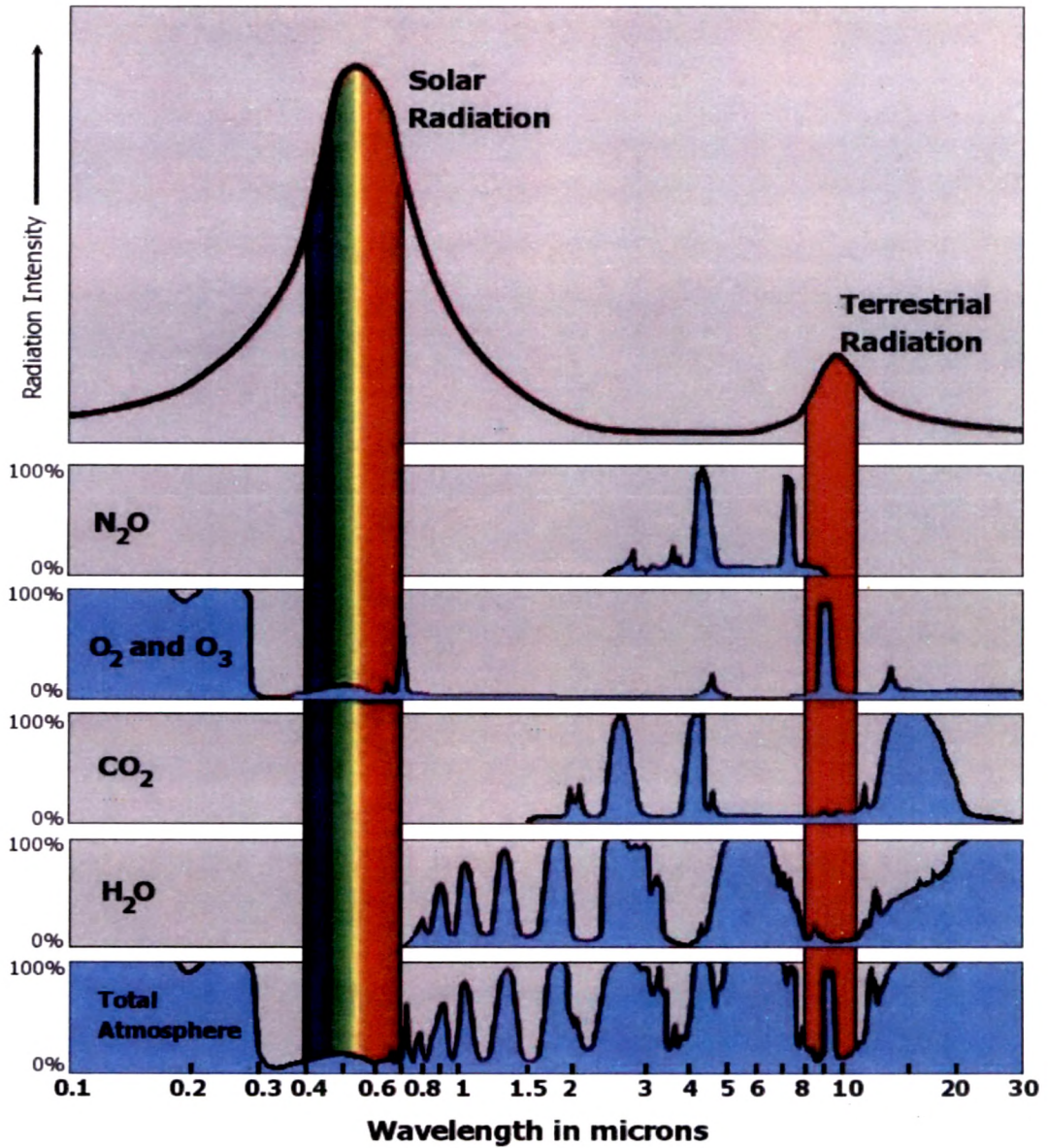


Figure 2.11. Principal absorption features of different gases present in Earth's atmosphere (Hoffman and Simmons, 2008)

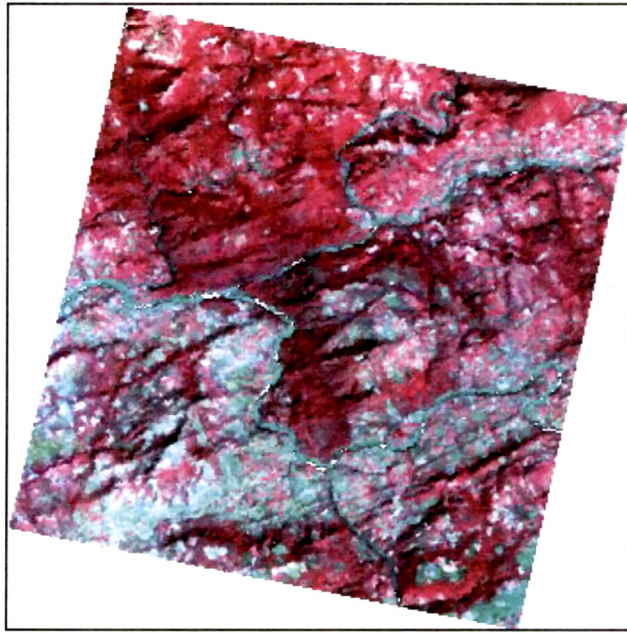


Figure 2.12. False colour composite of October Hyperion image subset

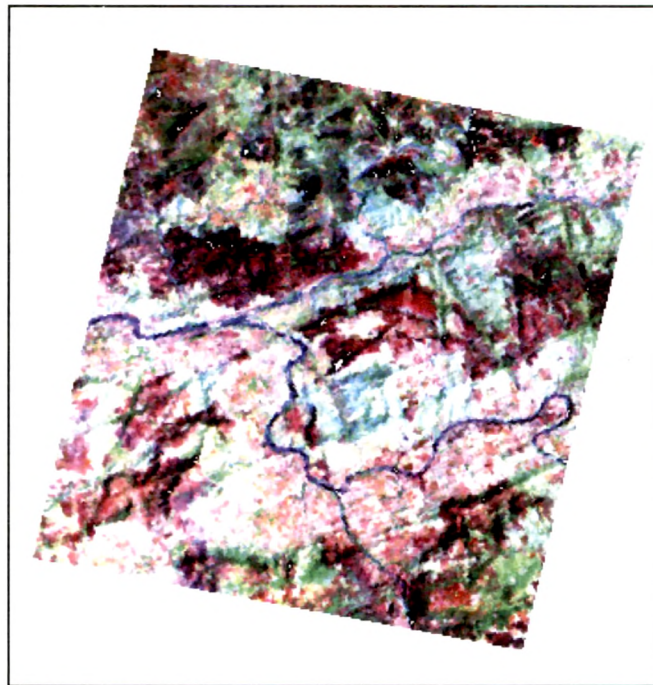
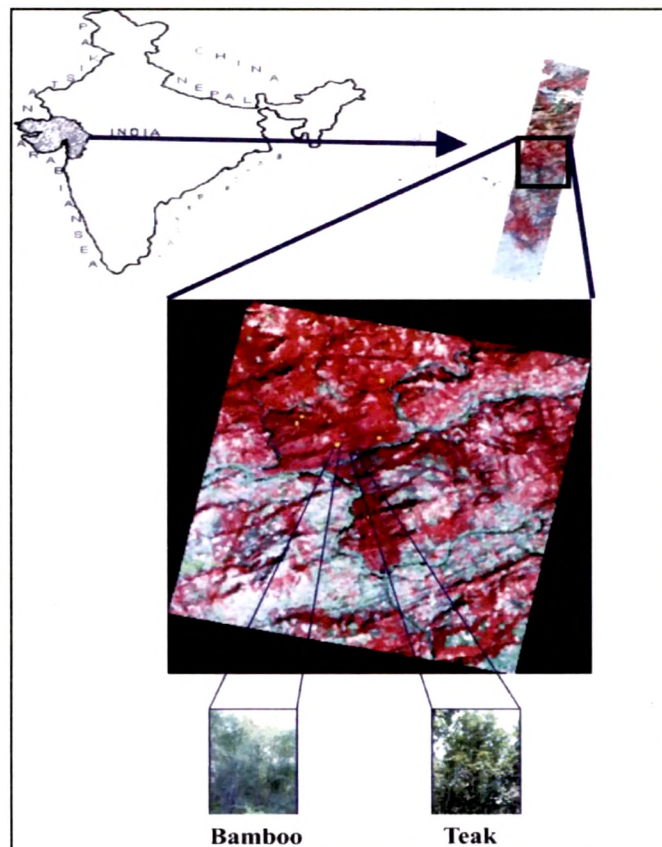


Figure 2.13. False colour composite of April Hyperion image subset

## 2.11 Field data collection

Quadrats of  $30 \times 30$  m size were marked across the study area (a subset of  $67.5 \text{ km}^2$ ). Ground control points (GCPs) were taken with the help of global positioning system receiver for each marked quadrat (Magellan<sup>®</sup> explorer 600, accuracy  $\pm 5$  m). Quadrats size coincides with spatial resolution of EO-1 (30m). Guidelines given by Sanchez-Azofeifa et al. (2005) were used for selection of patches (of teak, bamboo and mixed vegetation covers). Quadrats marked for each vegetation cover fall in a patch size of  $3 \times 3$  pixel window. A total of 100 quadrats (35 of teak, 35 for bamboo and 30 for mixed vegetation cover) were laid down (**Figure 2.14**). Number of quadrats laid down for each cover is proportional to field occupancy. Nearly 15 % of the Hyperion image subset was covered in the field survey. Sampling period coincides with that of satellite data acquisition. Density of trees in each quadrat was measured.



**Figure 2.14. Distribution pattern of teak and bamboo quadrats in the image subset**

## **2.12 Measurement of attributes**

Biophysical and biochemical attributes of the three vegetation covers were recorded. Biophysical parameters such as density, diameter at breast height (DBH), height of the tree, specific leaf area (SLA), LAI, bole biomass, and canopy spread were measured. Total chlorophyll, nitrogen, lignin, cellulose, and water content were measured as biochemical attributes. Homogeneity in the vegetation cover of teak and bamboo made it possible to measure all these parameters in these two covers. Heterogeneity was a major limitation in mixed cover for monitoring all these parameters with same level of precision. Hence, only bole biomass and canopy spread were measured.

## **2.13 Measurement of biophysical attributes**

### ***LAI measurements***

Litter trap method was used to estimate leaf area of Teak and Bamboo (for details please refer Vyas et al., 2010). Briefly, fallen leaf litter was collected from ten 900 m<sup>2</sup> plots in pure patches of Teak and Bamboo. In each plot litter traps of 1×1 m size (8 in number) were laid down randomly (Litter traps cover 8 m<sup>2</sup> surface area in each plot). Collected foliage litter was dried (at 70 °C for 48 h) and weighed to compute the dry mass of litter. Extreme values were discarded. Mean values (g m<sup>-2</sup>) were obtained from readings of each plot. Total weight of the leaves fallen under canopy area of each tree was calculated. Leaf dry weight was converted into leaf area by multiplying value with specific leaf area (SLA, calculated as leaf area per unit leaf dry mass). Independently 15-20 mature leaves of both the species were plucked from five trees with different canopy spread areas. Leaf area and dry weights of these leaves were measured. Subsequently mean specific leaf area (Leaf area/ dry weight of leaf) for both the species was calculated. Leaf area of all the individuals (either of Teak or of Bamboo) present in a 30×30 m quadrat was obtained by multiplying average of leaf area of sampled tree with density of trees in quadrat. LAI for each quadrat was subsequently calculated.

Regression equations were developed between Leaf area (LA) calculated from litter trap method and canopy area for teak and bamboo trees (n=10). These regression equations were used for estimation of LA of all other quadrats of teak and bamboo.

### **2.13.1. Bole biomass measurements**

Biomass of the main trunk / bole was measured. In each sampled quadrat, tree height and diameter at breast height (DBH) of each tree were measured. Tree height and DBH were measured by clinometers and tree Calipers. They were classified into respective diameter and height classes. DBH and height of trees were used for the computation of standing bole biomass. Volume and weight were measured from logs of each species (n=10). Wood density was measured as a ratio between volume and weight of that log. Biomass equation developed by Overman et al., (1994) for tropical tree species was used to compute the bole biomass of the trees ( $DBH^2 \times \text{height} \times \text{wood density}$ ). Bole biomass of all the trees in a quadrat was summed up to obtain total bole biomass of quadrat. This procedure was carried out in quadrats occupied by teak and mixed vegetation cover. Biomass of quadrats occupied by bamboo was measured differently. In each quadrat there were many bamboo coups and each coup was made up of many individual clumps. Number of clumps in each coup was counted. 5-6 representative clumps were identified. DBH and height were measured. Biomass of each clump was measured (Overman et al., 1994). Average biomass of a clump was calculated. Subsequently biomass of each coup was obtained (Average biomass of clumps  $\times$  number of clumps in a coup). This procedure was repeated for 20 coups of different sizes. Mean biomass was calculated. This was extrapolated to calculate biomass of a quadrat occupied by bamboo (a mean biomass of the coup  $\times$  number of coups in the quadrat). Bole biomass of mixed vegetation cover was estimated using the equation coined by Brown et al., (1989) for dry forests of India.

### **2.13.2 Canopy area**

From each sampled quadrat 10 individuals of different girth (small/medium/large) were marked. Spread of canopy in 4 directions was measured for each individual for keeping each individual keeping trunk as the center. Canopy area of each individual was calculated using mean value of radius. Canopy area of the quadrat was extrapolated (mean canopy area of the individual × density of trees in quadrat).

## **2.14 Measurement of biochemical attributes**

### **2.14.1 Foliage sampling**

Foliage was collected randomly from different parts of the canopy of teak and bamboo. All the leaf samples collected for analysis represent different hues and conditions naturally found in leaves. Leaves (n=20) were collected from individuals of different girth classes for analysis.

### **2.14.2 Chlorophyll measurements**

1 cm<sup>2</sup> leaf discs were cut from each leaf and chlorophyll was extracted in Dimethyl sulphoxide (DMSO). Extractants were centrifuged and the precipitants were again extracted in DMSO. This process was repeated till the samples became pale in color. Supernatants were pooled. Spectrophotometer readings (Perkin Elmer ® UV- visible) were taken and total chlorophyll was measured (Arnon, 1949). Mean chlorophyll values (g m<sup>-2</sup>) coming from all the samples of a quadrat were extrapolated to get the chlorophyll content of a quadrat (Mean chlorophyll per unit area × Total leaf area of the quadrat).

$$\text{Total chlorophyll} = [27.8 \times A_{645\text{nm}}] \times [V/ 100 \times W \times A]$$

**A= absorbance at 645 nm**

**V= final volume**

**W= fresh weight of sample (g)**

**A= path length (1 cm<sup>2</sup>)**

(Chlorophyll content was expressed as g m<sup>-2</sup>)

### **2.14.3 Nitrogen, Lignin and Cellulose measurements**

Collected leaf samples were oven dried at 70 °C for 48 hours and grinded. Dried leaf powder was then used for the estimation of nitrogen, lignin and cellulose. Nitrogen was estimated with the help of CHN analyzer (PERKIN ELMER®, Series II, 2400). Lignin and cellulose were estimated by the method of Booker et al. (1996). Powdered samples were coming from leaves of different hues and levels of maturity as seen on the canopy. For each measurement number of samples taken were twenty (n= 20). Utilizing these readings mean values were calculated, extrapolated to g m<sup>-2</sup>. Subsequently they were projected to obtain values for sampled quadrats (mean value per unit area × total leaf area of the quadrats). Logs were acquired for teak trees for estimation of lignin and cellulose content in. Dried wood powder was obtained from different points across the diameter of logs. This wood powder was used for estimation of lignin and cellulose. Mean values (n=20) of lignin and cellulose (g Kg<sup>-1</sup>) were extrapolated to get the respective parameter content of a quadrat (mean lignin or cellulose content × total bole biomass of a quadrat). For bamboo, instead of log pieces, bamboo clumps were used to obtain dried powder. Rest of the protocol remained the same.

### **2.14.4 Water content measurements**

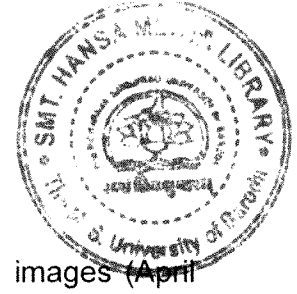
Fresh weights of collected mature leaf samples were measured. These were oven dried at 70 °C for 48 hours and subsequently dry weights were measured. The leaf water content per unit leaf area or Equivalent Water Thickness (EWT) was measured as the ratio between the quantity of water and the leaf area (Ceccato et al., 2001). EWT corresponds to a hypothetical thickness of single layer of water averaged over the whole leaf area (Danson et al., 1992). Mean measured EWT (g m<sup>-2</sup>) coming from all the samples were extrapolated to get the EWT of a quadrat (mean EWT per unit area × Total leaf area of the quadrat).

$$\text{EWT} = \text{FW} - \text{DW} / \text{A}$$

**Where, FW = Fresh weight of leaf**

**DW = Dry weight of leaf**

**A = Leaf area**



## 2.15 Acquisition of reflectance spectra

GCPs taken for all the quadrats were transferred to Hyperion images (April and October). Hyperion reflectance spectra coming from 3×3 pixel window around marked quadrats were averaged to obtain reflectance spectra of each quadrat of teak and bamboo.

## 2.16 Laboratory spectra

Laboratory spectra of teak and bamboo along with few important mixed vegetation tree species (*Madhuca*, *Mangifera*, *Ficus*) were obtained using foliage samples collected from the field. All leaves collected in the field were placed in plastic bags and kept in cool condition until they were subjected for spectral measurements. Reflectance spectra coming from 10 leaves (young, middle and mature ones) of all the species were averaged to get standardized leaf reflectance spectra for further analysis (total 3 different standardized spectra for five species, n=15). All spectral measurements were made with a field portable spectrometer (ASD FieldSpec<sup>®</sup>3). The FieldSpec<sup>®</sup>3 has a spectral range from 350 to 2500 nm with 1 nm bandwidth. Leaf illumination was provided through halogen lamp. Leaf thickness readings and quantification of pigments (total chlorophyll and chlorophyll a, b) were done for the same leaf samples and averaged readings were taken (n=15). Leaves of selected species for laboratory spectra acquisition showed variation in various attributes (leaf thickness, pigmentation). Stepwise Discriminant Analysis (SDA) was carried out to find out wavelengths showing difference in reflectance due to variations in leaves. Laboratory spectra obtained for above mentioned species were compared with stand level Hyperion reflectance spectra for the same species. Indices derived by other researchers were tested for their performance in estimation of total chlorophyll, chlorophyll a and chlorophyll b from laboratory spectra (**Table 2.2**).

$$\text{Total chlorophyll} = [(27.8 \times A_{645\text{nm}}) / 1000] \times \text{final volume in ml.}$$

$$\text{Chlorophyll a} = [(12.3 \times A_{663\text{nm}}) - (0.86 \times A_{645\text{nm}}) / 1000] \times \text{final volume in ml.}$$

$$\text{Chlorophyll b} = [(19.3 \times A_{645\text{nm}}) - (3.6 \times A_{663\text{nm}}) / 1000] \times \text{final volume in ml.}$$

**Table 2.2. List of Indices tested for estimation of total Chlorophyll, chlorophyll a and b from laboratory spectra**

Index	Computation	Reference
SAVI (Soil Adjusted Vegetation Index)	$(R_n - R_r) (1+L) / (R_n + R_r + L)$ where $L = 0.5$	Huete, (1988)
MSAVI2 (Modified SAVI)	$R_n + 0.5 - ((R_n + 0.5)^2 - 2 (R_n - R_r))^{0.5}$	Qi et al., (1994)
OSAVI (Optimized SAVI)	$(1+0.16) (R_{800} - R_{670}) / (R_{800} + R_{670} + 0.16)$	Rondeaux et al. (1996).
MSR (Modified SR)	$MSR = ((R_{800} - R_{670}) - 1) / ((R_{800} + R_{670})^{0.5} + 1)$	Chen (1996)
RDVI (Renormalized Difference Vegetation Index)	$RDVI = (R_{800} - R_{670}) / (R_{800} + R_{670})^{0.5}$	Rougean and Breon, (1995)
MCARI (Modified CARI)	$MCARI = [(R_{700} - R_{670}) - 0.2(R_{700} - R_{550})] (R_{700}/R_{670})$	Daughtry et al., (2000)
TCARI (Transformed CARI)	$TCARI = 3 [(R_{700} - R_{670}) - 0.2(R_{700} - R_{550}) (R_{700}/R_{670})]$	Haboudane et al., (2002)
TVI (Triangular vegetation index)	$TVI = 0.5 [120 (R_{750} - R_{550}) - 200 (R_{670} - R_{550})]$	Broge and Leblanc (2000)
SIPI (Structural insensitive pigment index)	$SIPI = (R_{800} - R_{445}) / (R_{800} + R_{680})$	Penuelas et al., (1995)
NPCI (Normalized Pigment Chlorophyll Index)	$NPCI = (R_{680} - R_{430}) / (R_{680} + R_{430})$	Penuelas et al., (1995)
MCARI1	$MCARI1 = 1.2 [2.5 (R_{800} - R_{670}) - 1.3 (R_{800} - R_{550})]$	Haboudane et al., (2004)
MCARI2	$MCARI2 = 1.5 [2.5 (R_{800} - R_{670}) - 1.3 (R_{800} - R_{550}) / [(2 R_{800} + 1)^2 - (6R_{800} - 5 (R_{670})^{0.5}) - 0.5]$	Haboudane et al., (2004)
Red edge 750~700	$R_{750} - R_{700}$	Gitelson and Merzylak (1997)
Red edge 740~720	$R_{740} - R_{720}$	Vogelmann et al., (1993)
ZTM (Zarco Tejada and Miller)	$ZTM = (R_{750} / R_{710})$	Zarco Tejada et al., (2001)

## 2.17 Data analysis

Stepwise Discriminant Analysis (SDA) was carried out to find out optimal wavebands to discriminate different vegetation classes. Discriminant analysis categorizes samples using multivariate separability measures such as Wilks' lambda (Thenkabail, 2002). Wilks' lambda ( $L$ ) is given by (Green and Carroll, 1978).

$$\Lambda = \frac{|S_{effect}|}{|S_{effect}| + |S_{error}|}$$

Where,  $S$  is a matrix which is also known as Sum of Squares and Cross-Products (SSCP). Wilks' Lambda is a multivariate test of significance and

ranges between 0 to 1. The values of Wilks' lambda are indicative of separability or discriminatory power of spectral wavebands. The values close to 0 indicate that the group means are different and values close to 1 indicate that they are not different and 1 indicates all means are the same. The band selection process stops, when there no further significant decrease in Wilks' lambda value. The bands selected through this analysis were used for classification. In present study Hyperion reflectance spectra of pixels marked as training sites were subjected for stepwise discriminant analysis (SPSS V11.5 software). Inherent supervised classification mechanism from ENVI V 4.6 was used to cluster pixels in the dataset into classes corresponding to defined training classes. Built in complex non-linear classifications algorithms (Artificial Neural Network, ANN and Spectral Angle Mapper, SAM, Support Vector Machine, SVM) from ENVI V.4.6 were used to classify image. All the three classifiers were tested to classify spectra coming from selected bands (from SDA) and also for whole spectra (Coming from all 165 bands).

SAM is a spectral matching technique (Kruse et al., 1993). It is a physically-based spectral classification that uses a n-dimensional angle to match pixel spectrum to reference spectrum. SAM classification was accomplished by assigning each sample spectrum to the class with the closest similarity. Maximum angle threshold for class separation was 0.10 radians.

The Support Vector Machine (SVM) is an effective distribution free classifier that has been widely used in the recent years for solving hyperspectral classification problems (Camps-Valls and Bruzzone, 2005). Another classifier tested was SVM inbuilt in ENVI V.4.6. ENVI has a number of options in kernel selection such as Linear, Polynomial, Sigmoid and Radial Basis function (RBF) for SVM. In present study the Hyperion image were classified with each of these kernels. Kernel methods exploit information about the inner products between data items. RBF was chosen for its accuracy in classification (**Figure 2.15**). Different combinations of penalization constant (C) and kernel parameters were tested. Accuracy values obtained for all tested combinations were in the range of 60-70% (for 22 bands) and 70-80% (for 165 bands). Combination with highest accuracy was considered.

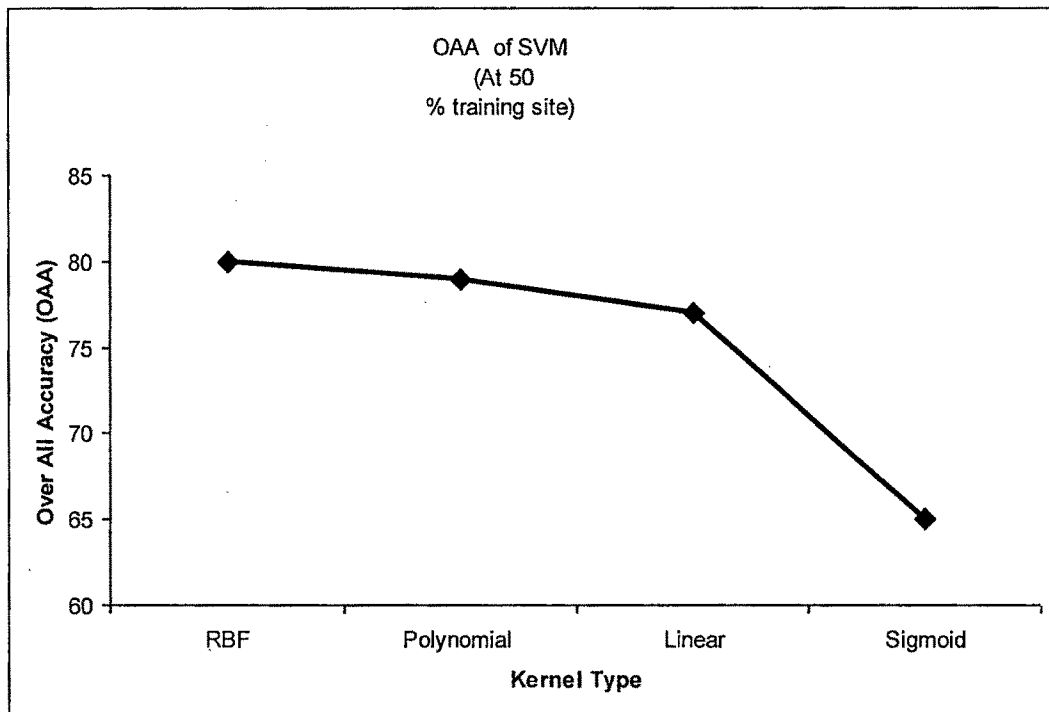


**Figure 2.15. Performance of SVM classifier for different Kernel types**

ANN is the most widely used model and its design consists of one input layer, at least one hidden layer and one output layer. In present study for ANN one hidden layer and logistic method for back propagation were selected. We have classified image with the help of different iterations (1000-10000). Image processing was finally done with 5000 iterations.

Hits from the all correctly classified pixels were used for accuracy assessment. Two measures of classification accuracy (user's and producer's accuracy), overall accuracy (OAA) and kappa coefficient were calculated (Congalton, 1991; de Leeuw et al., 2006; Foody, 2002).

In this study Partial Least Square (PLS) regression analysis was done to determine the relative contribution of each biochemical and biophysical parameter to the Hyperion reflectance spectra. PLS was used as it has proven to be the most successful practical approach for prediction of foliar properties from airborne or space-borne hyperspectral data (Asner and Martin 2008; Martin et al. 2008; Smith et al. 2003, 2002). The partial least squares

(PLS) regression was developed by Wold in the late 1960s for econometrics (Wold, 2001) and then introduced as a tool to analyze data from chemical applications in the late 1970s (Geladi and Kowalski, 1986; Martens et al. 1989). An introduction and a statistical overview of PLS regression can be found in Geladi and Kowalski (1986) and Wold et al. (2001). This technique is an extension of multiple regression analysis in which the effects of linear combinations of several predictors on a response variable (or multiple response variables) are analyzed. Associations are established with latent factors extracted from predictor variables that maximize the explained variance in the dependent variables.

As with other linear calibration methods, in PLS regression also the aim is to build a linear model:

$$Y = X \beta + \varepsilon$$

Where,  $Y$  is the mean-centered vector of the response variable (vegetation attributes),  $X$  is the mean-centered matrix of the predictor (Hyperion reflectance spectra),  $\beta$  is the matrix of coefficients, and  $\varepsilon$  is the matrix of residuals.

Reflectance spectra acquired from October Hyperion image were utilized for estimating biochemical attributes (chlorophyll, nitrogen, lignin, cellulose and EWT) at canopy level. Reflectance spectra of April Hyperion image were tested for estimating major biochemical constituents of stem (lignin and cellulose). PLS regression analysis was done to determine the relative contribution of each biochemical and biophysical parameter to the Hyperion reflectance spectra. Leave One Out Cross Validation (LOO-CV) method was used to select the optimal number of PLS factors or latent variables to be included in the regression models (Geladi and Kowalski, 1986; Viscarra Rossel, 2005). Factor loadings were mentioned in **Table 2.3**. PLS regression analysis was performed using Unscrambler X software. Analysis was performed using the entire spectra (165 bands). PLS regression models were

also developed for selected spectral regions sensitive to a specific attribute. Selection of spectral regions was based on sensitive wavelengths recognized by other researchers for different biochemical and biophysical attributes (**Appendix A**). To make the distribution of LAI data normal, data values of both the species were combined and PLS analysis was carried out. For all PLS regression models Standard Error calibration (SEC) and Standard error of cross validation (SECV) values were generated by LOO-CV. Highly sensitive wavelengths from best performing PLS regression model for chlorophyll and LAI were selected for vegetation index development. Simple and Normalized difference (ND) vegetation indices were developed. LOO-CV technique was used for validation of developed models. Vegetation indices giving best results were recognized for the development of linear regression models for the quantification of chlorophyll and LAI. Prediction error of vegetation indices from present study were compared with prediction errors obtained from other studies.

**Table 2.3. Factor loadings for PLS model generation**

	Parameter	(Factor loadings)	
		Full (teak/bamboo)	Subset (teak/bamboo)
1	Chlorophyll	(2/2)	(2/2)
2	LAI	3	3
3	Water	(2/2)	(3/2)
4	Nitrogen	(3/2)	(2/2)
5	Canopy area	(2/2)	(2/2)
6	Lignin (stem)	(2/2)	(2/2)
7	Cellulose (stem)	(2/2)	(2/2)
8	Lignin (foliage)	(2/2)	(2/6)
9	Cellulose (foliage)	(2/2)	(2/2)
10	Biomass	(2/6)	(3/3)